RADIATION DETECTION AND MEASUREMENT IN FLASH TUNNEL

Bhaskar Mukherjee

LLRF Group

FLASH SEMINAR

Deutsches Elektronen-Synchrotron

06-06-06

THE MAIN AIMS OF RADIATION DETECTION AND MEASUREMENT

160m long, 750 MeV Superconducting Electron Linac Driving the Vacuum UV-Free Electron Laser: FLASH

Characterisation of Linac Radiation Fields

Radiation Field Simulation (Isotopic Sources)

Radiation Field Assessment (Dosimetry)

Investigation of Radiation Effects on selected Commercial off the shelf (COTS) electronic components

Development of radiation effect Mitigation Techniques

MAIN CONTRIBUTERS OF THIS VENTURE
(in alphabetical order)

Dipl. Ing. Arkadeuz Kalicki, TU Warsaw
M.Sc. Thesis (completed) Topic: ***Radiation Effects on Optoelectronics***

Grad. Ing. Krzysztof Korzunowicz, TU Warsaw
B.Sc. Thesis (completed) Topic: ***Application of Genetic Algorithm, Neural Nets***

Dipl. Ing. Dariusz Makowski, TU Lodz
PhD Thesis (completed) Topic: ***Development of Radiation-Tolerant Microelectronics, Neutron and Photon Detectors for FLASH***

Dipl. Ing. Dominik Rybka, TU Warsaw
M.Sc. Thesis (completed) Topic: ***Radiation Effects on FPGA, Optoelectronics, DSP***
PhD Thesis (on going) Topic: ***As above, with more depth, Development of Passive Radiation Detector for FLASH / XFEL***

RADIATION EFFECTS ON MICROELECTRONICS IN FLASH TUNNEL
(A Short Summary)

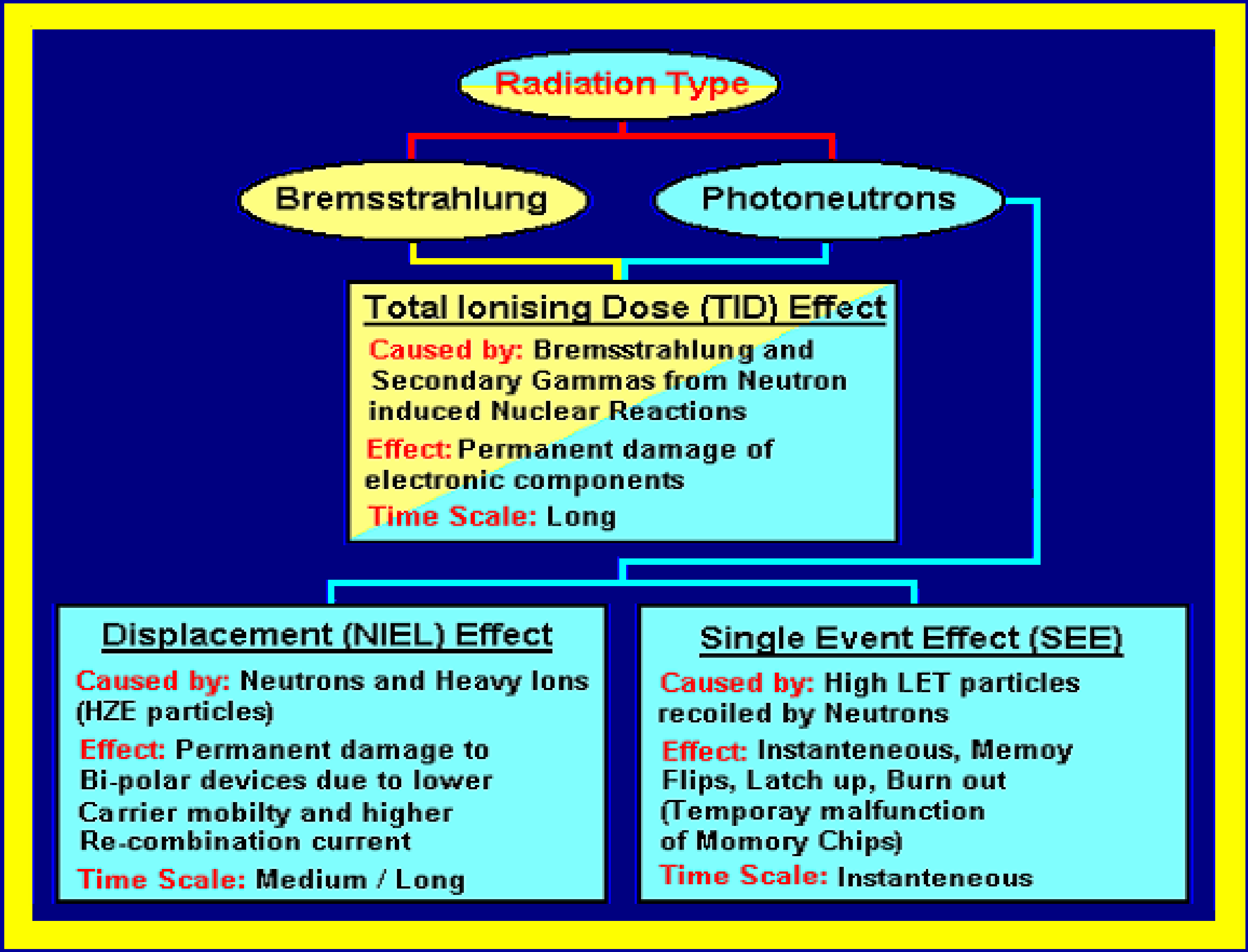

RADIATION SOURCE CHARACTERISAION IN FLASH TUNNEL

1) Gamma Rays (Bremsstrahlung)

2) Neutrons (GDR Photoneutrons)

1) ESTIMATION OF THE BREMSSTRAHLUNG ENERGY SPECTRUM IN FLASH TUNNEL

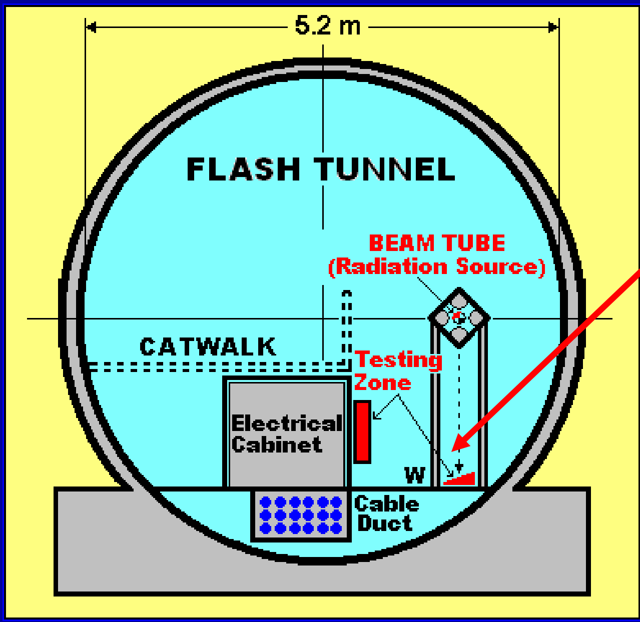

Cross Section of the FLASH tunnel
Testing Zone (Microelectronics)
W (Stepped Pb-wedge)

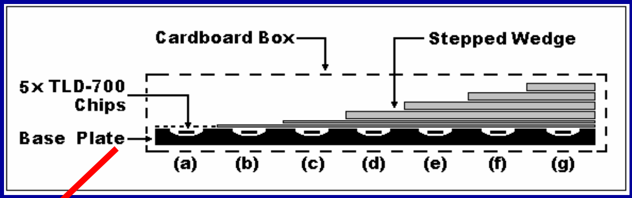

(1) Pb-wedge containing TLD 700* chips was exposed to BS generated in the Beam Tube.

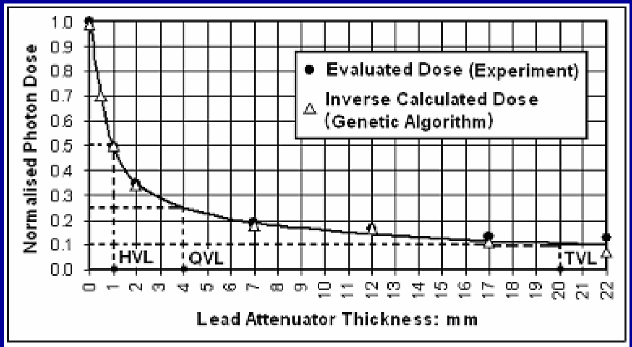

(2) TLD 700*s evaluated, Results plotted against Pb-width, HVL, QVL and TVL thicknesses of Pb were calculated.
*TL-105=> high neutron sensitivity =>under estimates attenuation => WRONG CHOICE

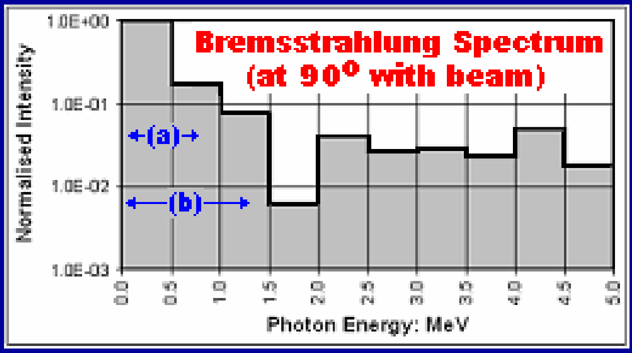

(3) Attenuation curve was analysed using a Genetic Algorithm to unfold the BS spectrum.

B. Mukherjee, S. Simrock, Appl. Radiat. Isot. (in print)

Results

E_G(peak) => 0.5 MeV
E_G(average) => 0.9 MeV

Comparison (Radioisotope Sources)

(a) ^{137}Cs => 0.67 MeV
(b) ^{60}Co => 1.3 MeV

2) NEUTRON ENERGY DISTRIBUTION IN FLASH TUNNEL

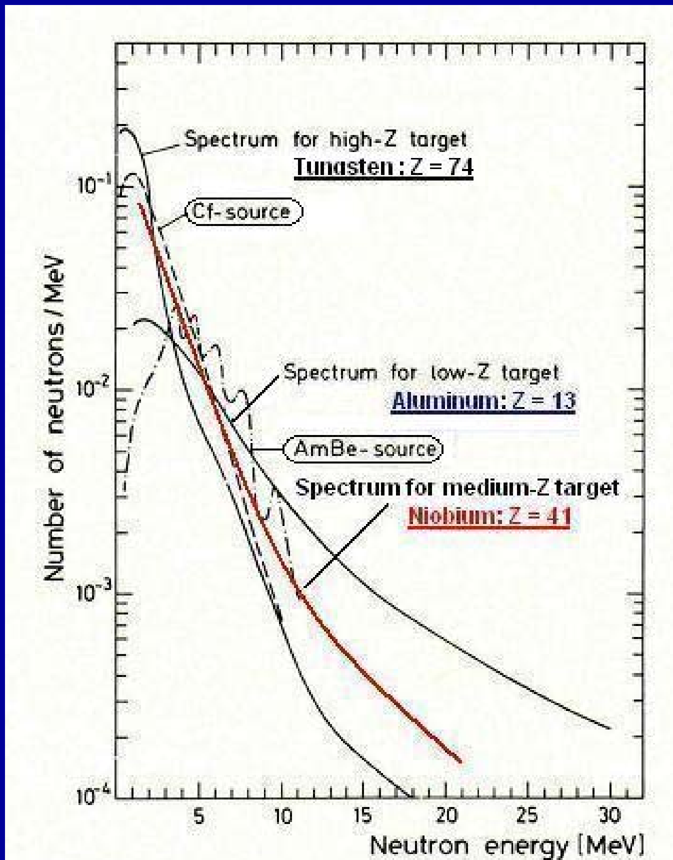

FIGURE 3 Spectral distributions of neutrons produced by one electron with an energy of 1 GeV. The spectra of radioactive neutron sources are shown for comparison.

K. Tesch, Particle Accelerator 9(1979)201

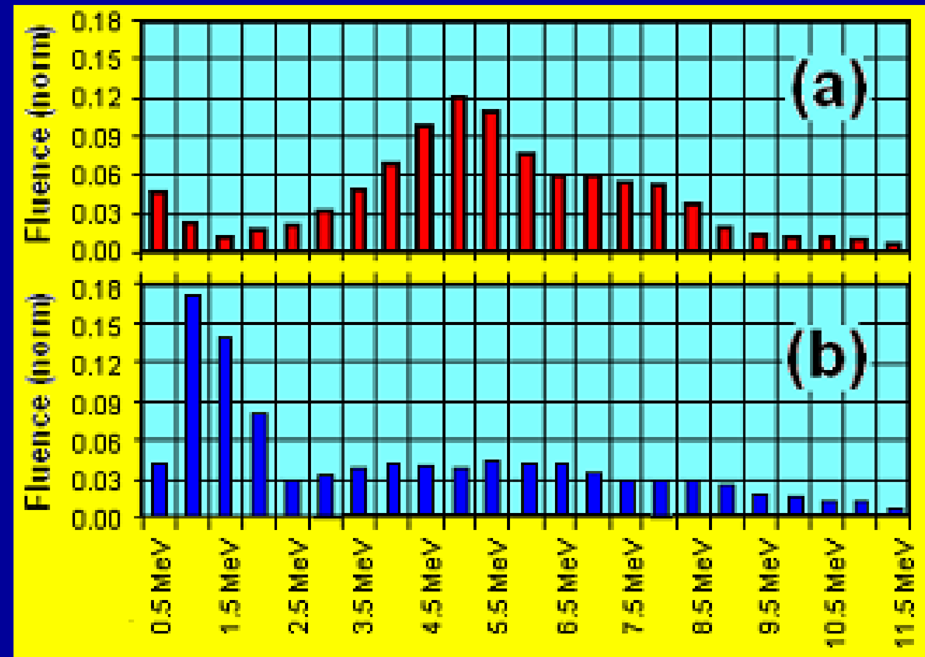

The Reference Neutron Spectra

(a) Un-moderated ^{241}Am/Be(α,n) , En (av) = 5.1 MeV

(b) Moderated with 6.9 cm H_2O, En (av) = 4.1 MeV

The areas under the histograms (a) and (b) are normalised to unity.

B. Mukherjee, Nucl. Instr. Meth. A363(1995)616

FINDINGS

A ^{60}Co source to simulate the FLASH Bremsstrahlung and could be used for calibration purposes

A $^{241}Am/Be$ source to simulate the FLASH Photoneutrons and could be used for calibration purposes

EXAMPLES OF TEST IRRADIATION

1) NEUTRON TEST IRRADIATION WITH ^{241}Am/Be SOURCE (Bare & Water Moderated)

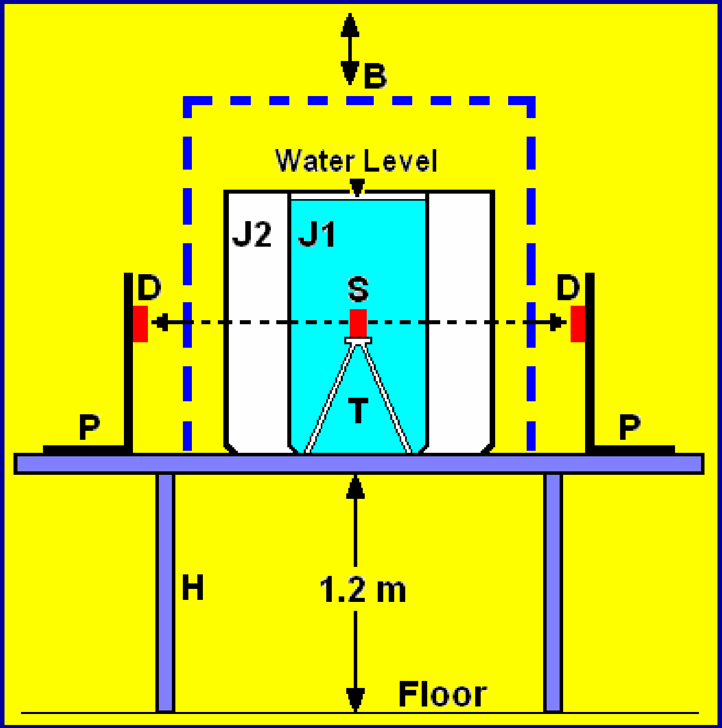

Legend

B: Thermal Neutron Shield (Borated Polyethylene)
D: Device under Test (DUT)
H: Table
J1, J2: Jars (16 and 33 cm radius respectively)
P: Stand
S: ^{241}Am-Be Neutron source
T: Tripod (Source holder)

Photograph of the neutron Irradiation device showing diverse types of DUT under irradiation.

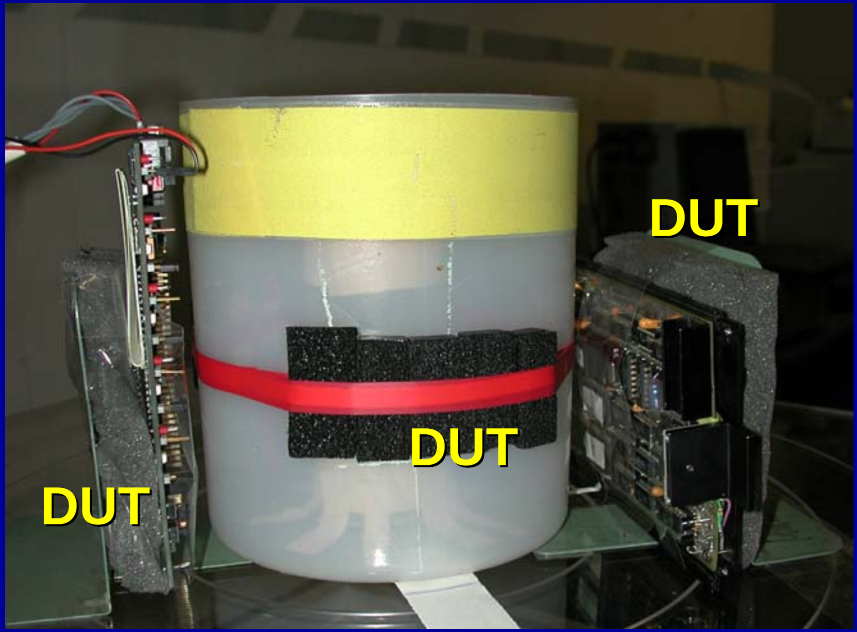

2) A DIGITAL SIGNAL PROCESSING (DSP) BOARD UNDER ^{60}Co-GAMMA IRRADIATION

TOOLS OF THE TRADE

1) Light Emitting Diodes (LED)

2) Thermoluminescence Dosimeter (TLD)

3) Bubble Detectors (BDPND)

4) Neutron Monitor based on SRAM (COTS)

1) GaAs LED as Passive Neutron Dosimeter

Displacement damage caused by fast neutrons in unbiased Gallium Arsenide (GaAs) Light Emitting Diodes (LED) resulted in a reduction of the light output.

On the other hand, a similar type of LED irradiated with gamma rays from a ^{60}Co source up to a dose level in excess of 1.0 kGy (1.0×10^5 rad) was found to show no significant drop of the light emission.

This phenomenon was used to develop a low cost passive fluence monitor and kerma dosemeter for accelerator-produced neutrons.

Neutron Irradiation Effects on Light Emission of LED

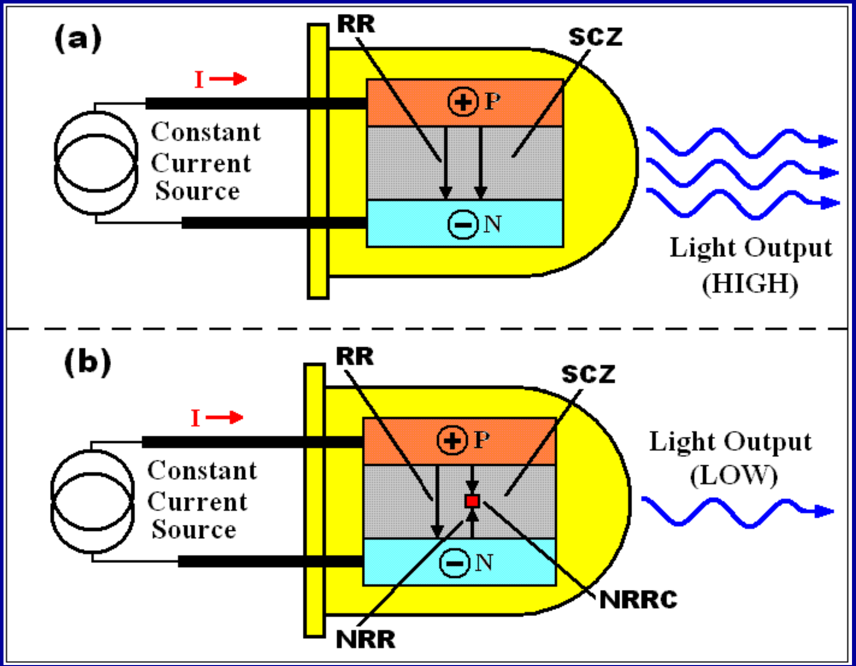

(a) Un-Irradiated (Control) LED:

All Electron/Hole pairs undergo radiative recombination (RR) in the space charge zone (SCZ)

Result: HIGH LIGHT OUTPUT

(b) LED Following Neutron Irradiation

Non radiative recombination centres (NRRC) are produced by Displacement Damage
Only a fraction of Electron/Hole pairs undergo Radiative Recombination (RR)
The rest is dissipated in the space charge zone by Non Radiative Recombination (NRR)

Result: LOW LIGHT OUTPUT

YELLOW GaAs LED USED IN OUR INVESTIGATIONS

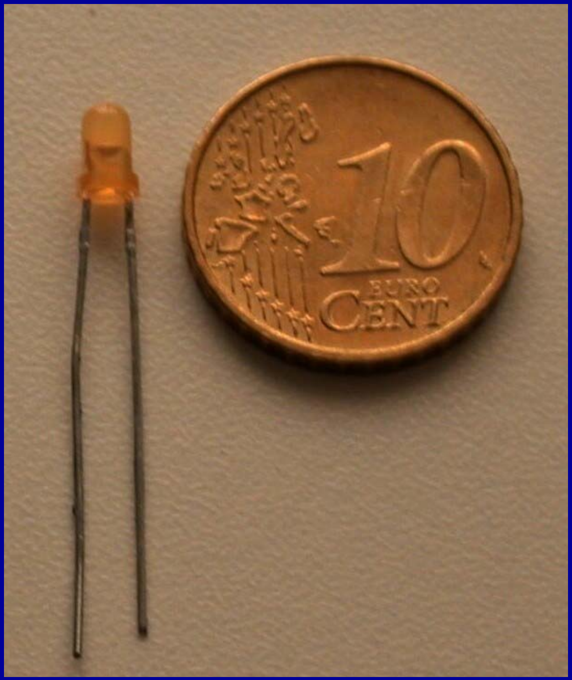

Manufacturer: ***Panasonic, Corp. Japan***
Model: ***LN 48YPX***
Maximum Fwd. current: ***20 mA***
Wave length of emitted light: ***6800 Angstrom***
Diameter: ***3 mm***
Length: ***5 mm***
Worth: ***approx. 10 cents***
Type: ***COTS***

We have evaluated the Light output (Lux) of the LED as a function of Fwd. current.

The optimum Fwd. current for the LED used as neutron dosimeter was set at 13.0 mA.

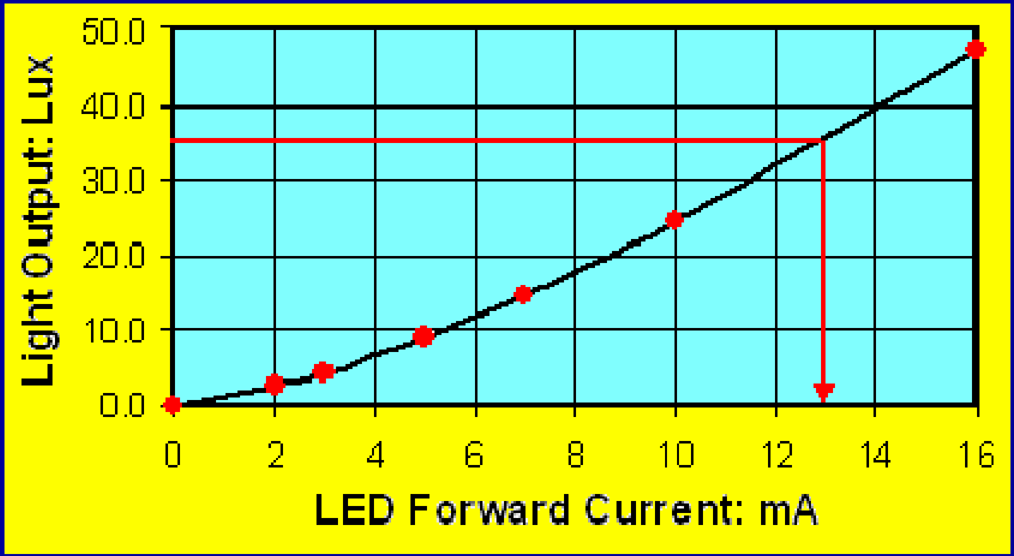

EXPERIMENTAL EVALUATION OF THE GaAs-LED SENSITIVITY FOR GAMMA RAYS AND NEUTRONS

Batches of GaAs-LED were irradiated with ^{60}Co Gamma rays (1.3 MeV) and ^{241}Am/Be (4.1 MeV) Neutrons. The light output of the LEDs were evaluated with the Digital Photometer described earlier. The relative (%) light output as functions Kerma in GaAs are plotted in the Figure shown below.

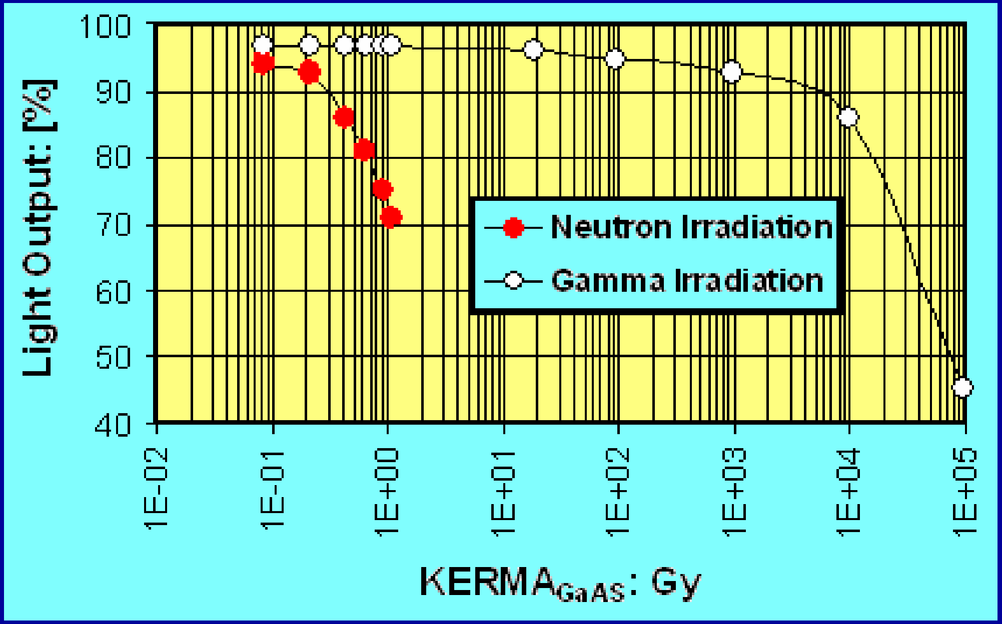

The results reveal that the fast neutrons possess > 4 orders of magnitude higher displacement damage producing capability in GaAs than gamma rays.

NEUTRON KERMA CALCULATION in GaAs

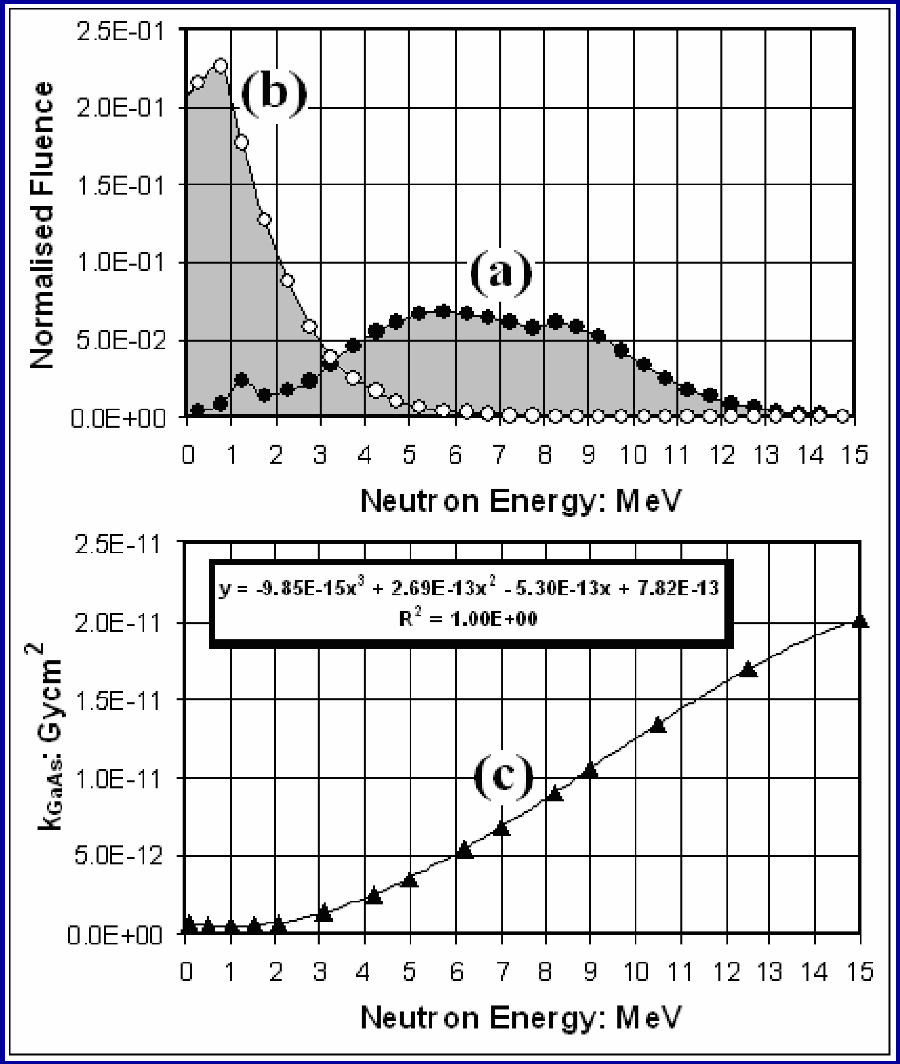

Showing the energy spectra of a ^{241}Am/Be neutron standard source (a) and the Giant dipole photo-neutrons produced by FLASH (b).

The integrated neutron fluence of both sources, i.e. the area (shaded) under the respective spectrum were normalised to unity.

The lower graph (c) displays the KERMA coefficient of GaAs (k_{GaAs}) as a function (the fitting polynomial is shown inset) of neutron energy.

The neutron KERMA is calculated by folding the KERMA coefficient (c) with the neutron fluence (a, b).

B. Mukherjee, D. Rybka, S. Simrock
Radiat. Prot. Dosim. (Submitted)

Fluence & Kerma Calibration Curves of LED Dosimeter

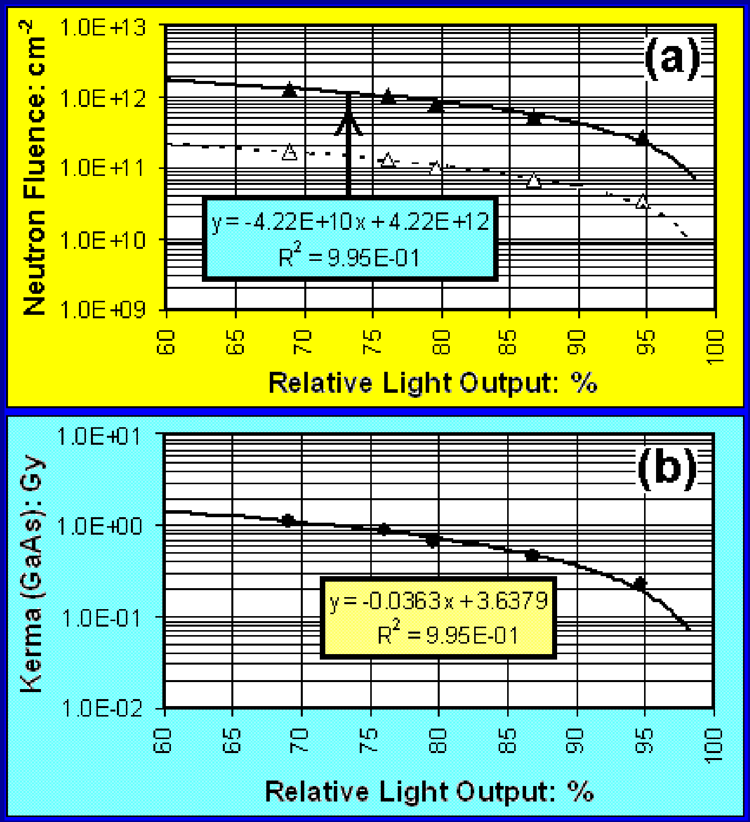

(a) Fluence Calibration

Hollow Triangles => ^{241}Am/Be Spectrum

Filled Triangles => Converted to GDR (FLASH) Spectrum, Fitting Polynomial inset

(b) Kerma Calibration

Independent of Spectral Distribution (Kerma is a SCALER)

2) Thermoluminescent Dosimeter

WE have purchased a portable battery operated TLD reader of PorTL originally developed for Space Dosimetry Applications by Hungarian Atomic Research Institute.

The PorTL system basically uses three different types of self calibrated (built in micro chip):

1) PorTL-E (^{Nat}LiF for Neutron dosimetry)
2) PorTL-G (^{7}LiF for *Medium Level* Gamma dosimetry)
3) PorTL-C (Al_2O_3-*Very Low Level* Gamma dosimetry)

We have used the PorTL Bulbs-G (^{7}LiF) to study the Radiation Induced Heat-Load-Effects in the Cryogenic System of the ACC 5

PorTL- THERMOLUMINESCENCE DOSIMETRY SYSTEM

PorTL Dosimeter Reader

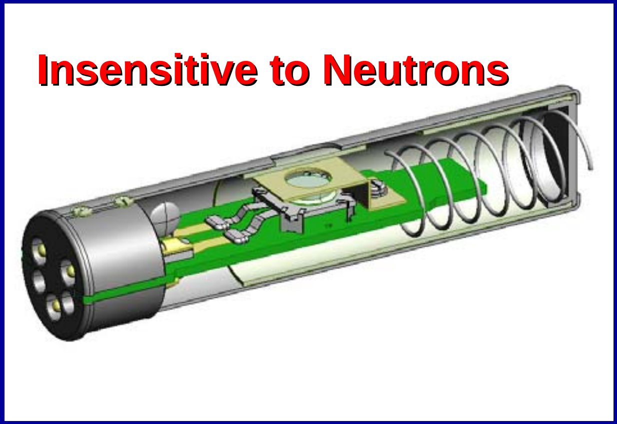

PorTL TLD (Al_2O_3) Bulb

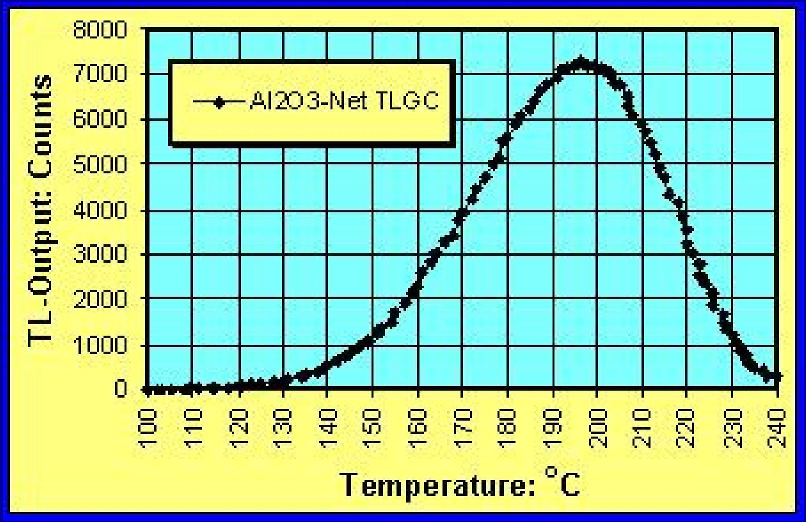

Typical Glow-Curve of a Al_2O_3 TLD-Bulb irradiated with gamma rays (745 micro Sv).

B. Mukherjee, A. C. Lucas. Radiat. Prot. Dosim. 47(1-4)(1993)177.
B. Mukherjee, D. Makowski, S. Simrock. Nucl. Instr. Meth. A545(2005)830.

3) Superheated Emulsion Bubble Detectors (BDPND)

(Ideally suited for Neutron Dosimetry with a strong gamma background)

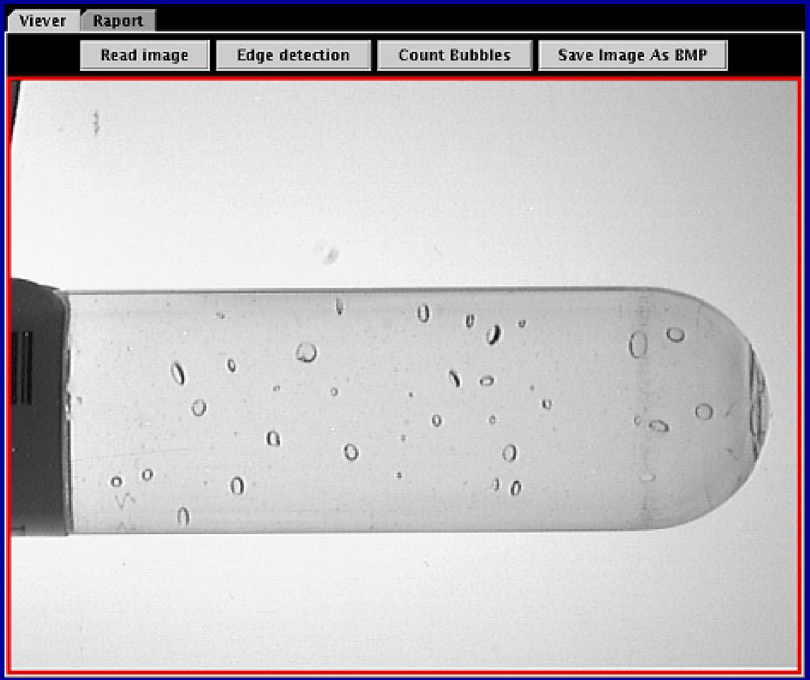

(a) Input: Digital photograph of the bubble dosimeter after neutron exposure

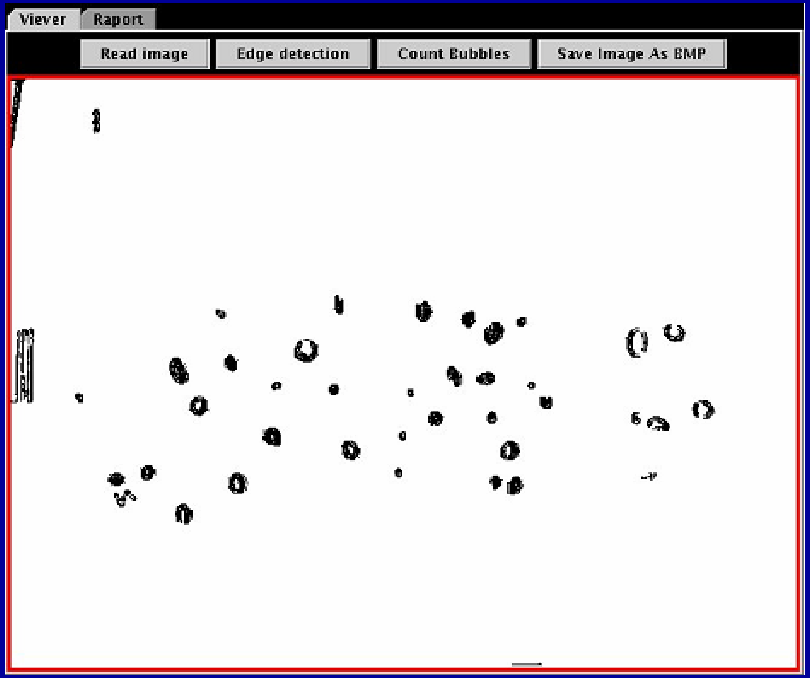

(a) Edge Detection
(b) Counting
(c) Data output

Automatic Bubble Counting Algorithm Results

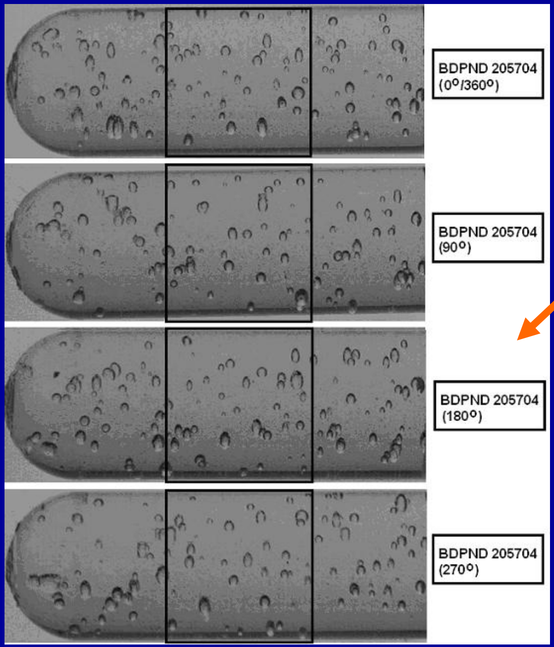

Original Photos

Filtered Photos
(OBCA-1)

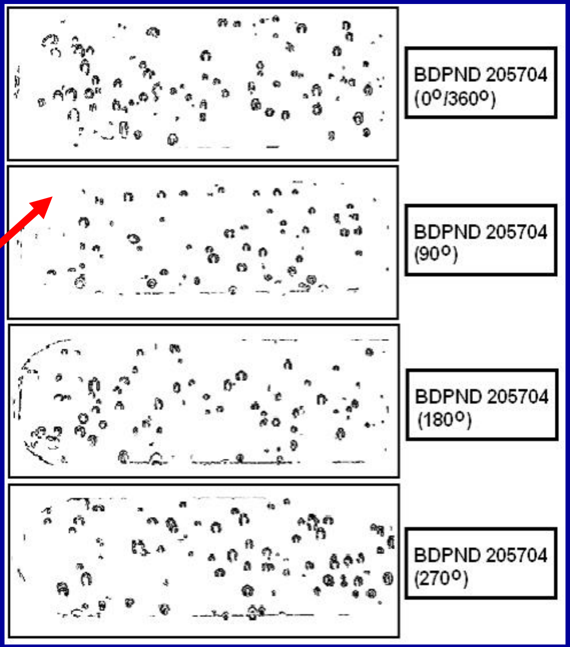

Bubble Count Results: (manual vs. OBCA)

	BDPND 205704
Neutron DE: [µSv]	50.6
Average Nr. of Bubbles (OBCA)	118.8
Average Nr. of Bubbles (Manual)	118.5
Sensitivity (OBCA) [µSv/Bubble]	0.426
Sensitivity (Manual) [µSv/Bubble]	0.427
Sensitivity (Supplier) [µSv/Bubble]	0.455

(A. Kalicki, TU Warsaw, M.Sc. Thesis, July 2004)

4) Static Random Access Memory (SRAM)

MECHANISM OF TRIGGERING A SEU

In a microelectronic circuit (M), embedded in the semiconductor substrate (S) a Single Event Upset (SEU) set off when the interacting ionising particle deposits sufficient energy in the sensitive volume enclosing the critical node (N). The SEU triggering mechanism could be divided in two broad categories:

(a) Direct Interaction

The high energy heavy (HZE) particle, i.e. of cosmic origin (P) directly interact with the critical node (N) by producing a track of electron/hole pairs, thereby causing the SEU.

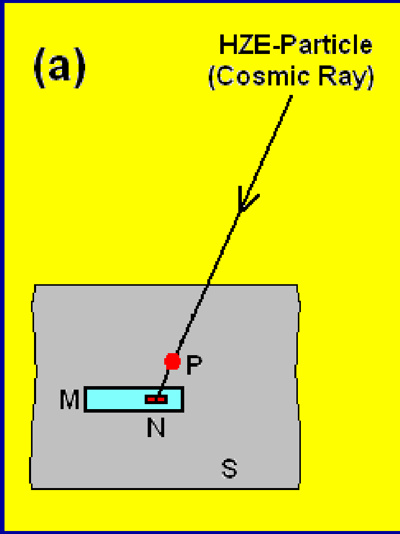

(b) Indirect Interaction

The primary particle, i.e. accelerator produced neutron undergo nuclear reaction with the primary atom (A) producing primary knockout atom (PKA) and secondary charged particle (CP), producing the SEU.

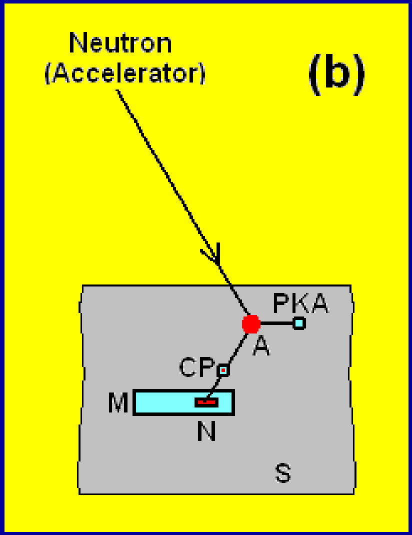

NEUTRON INDUCED NUCLEAR REACTIONS IN THE MICROCHIP

<u>Nuclear Reaction with Boron (1)</u>

Boron is used as a dopant and component of the glassification layer:

$^{10}B_5 + {^0n_1} = {^7Li_3} + {^4He_2}$ (1)
(Q = + 2.65 MeV)

<u>Nuclear Reactions with Silicon (2 & 3)</u>

Silicon is the major building block of all semiconductor devices:

$^{28}Si_{14} + {^0n_1} = {^{25}Mg_{12}} + {^4He_2}$ (2)
(Q = - 2.65 MeV)

$^{28}Si_{14} + {^0n_1} = {^{28}Al_{13}} + {^1H_1}$ (3)
Q = - 3.85 MeV)

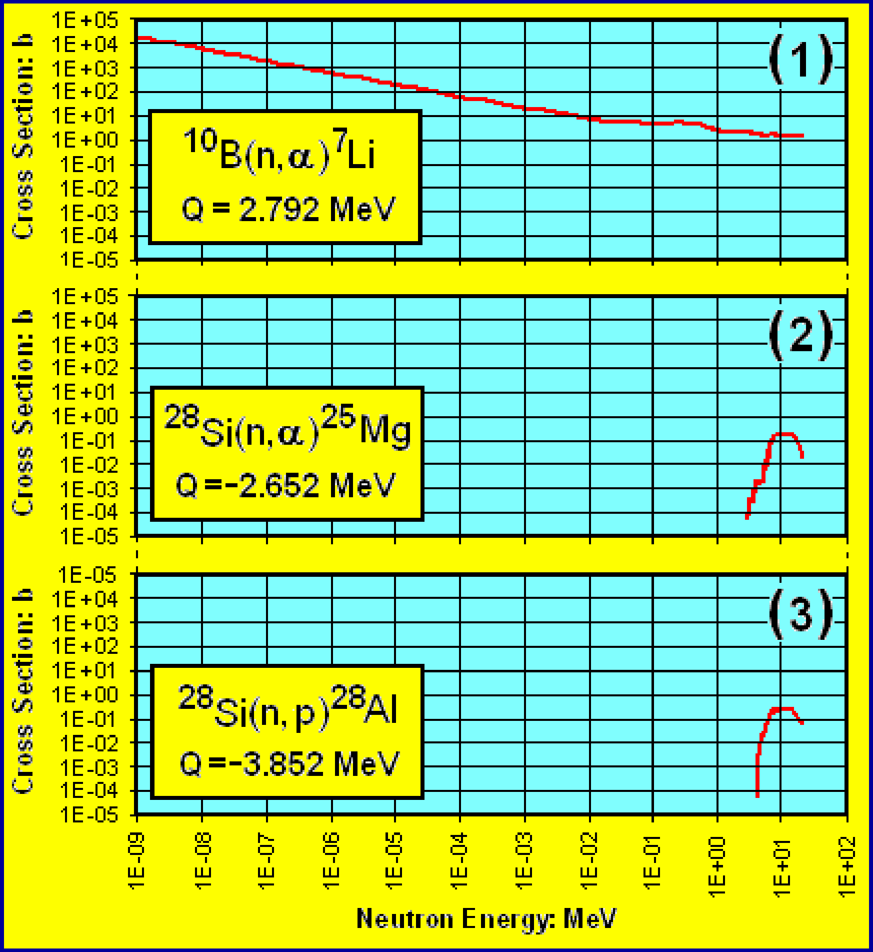

NEUTRON INDUCED NUCLEAR REACTIONS IN THE MICROCHIP (contd.)

Boron-10 ($^{10}B_5$) makes only 19.9% abundance in natural boron. However, due to very high *"exothermic"* reaction cross section of 3000 barn for thermal neutrons, the neutron capture reaction (1) overwhelms the *"endothermic"* (n, α) and (n, p) reactions (2 and 3) in Silicon (cross sections ca. 0.1 barn).

The physical properties of the reaction products of $^{10}B(n, \alpha)^7Li$ reaction are summarised in Table below.

Nuclear Reaction	React. Product	LET [MeV/mg/cm^2]	Range [micron]
$^{10}B(n, \alpha)^7Li$	^7Li	2.2	2.4
	^4He	1.1	5.0

Evidently, due to a higher range (5 micron) in silicon, the alpha particles (^4He) are the main candidate for triggering SEU in the microchip.

NEUTRON IRRADIATION OF SRAM CHIPS

512 kB non-volatile SRAM chips were irradiated with ^{241}Am-Be neutrons and stray neutrons existing in the FLASH tunnel.

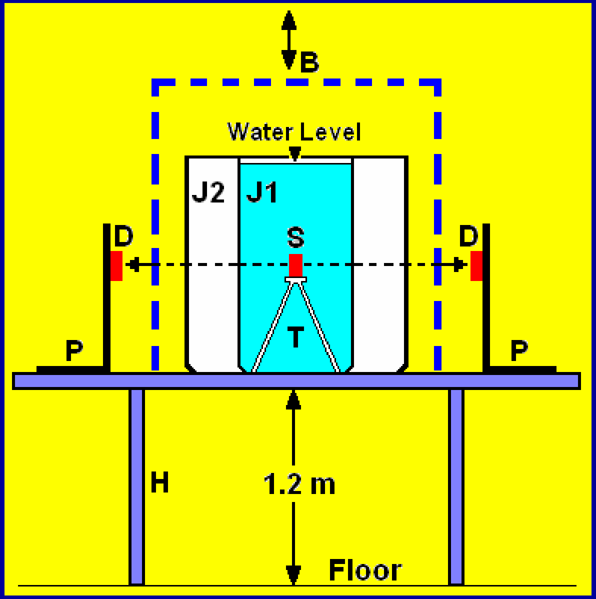

(1) ^{241}Am-Be Neutron Irradiation Device

B: Thermal Neutron Shield (Borated Polyethylene)
D: Device under Test (DUT)
H: Table
J1, J2: Jars (16 and 33 cm radius respectively)
P: Stand
S: ^{241}Am-Be Neutron source
T: Tripod (Source holder)

(2) In the FLASH (Electron Linac) Tunnel, warm side

C: Cable Duct
E: Electronic Instrument Cabinet
Q: Quadrupole Lens
S: SRAM Chips
W: Catwalk

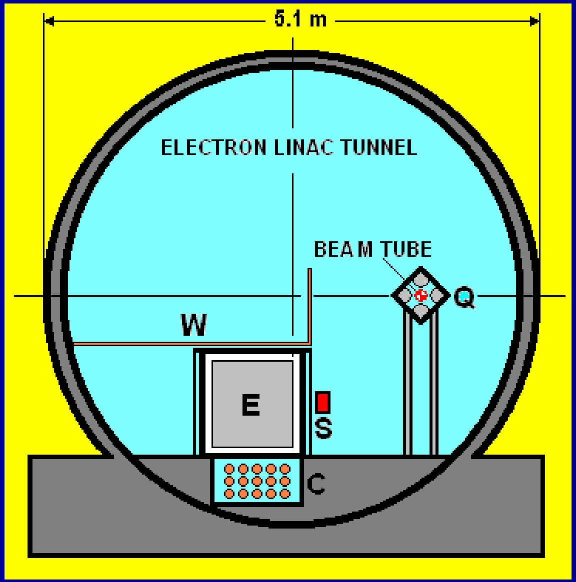

INTERPRETATION OF EXPERIMENTAL RESULTS

The number of SEU counted after neutron irradiation of the 512 kB SRAM chips are shown in the Table below:

SRAM Nr.	Irradiation Mode	SEU Counted
1	Am-Be (Bare)	40
2	Am-Be (Water Mod)	275
3	Am-Be (Water Mod + B-Shield)	19
4	Linac (Bare)	117
5	Linac (Polyeth. Mod)	619
6	Linac (Polyeth. Mod + B-Shield)	15

Poor Shield Material For SRAMs

The normalised SEU counts of the bare, polyethylene-moderated and shielded with Borated Polyethylene (Poly-Boron) sheet are shown

in the next Figure.

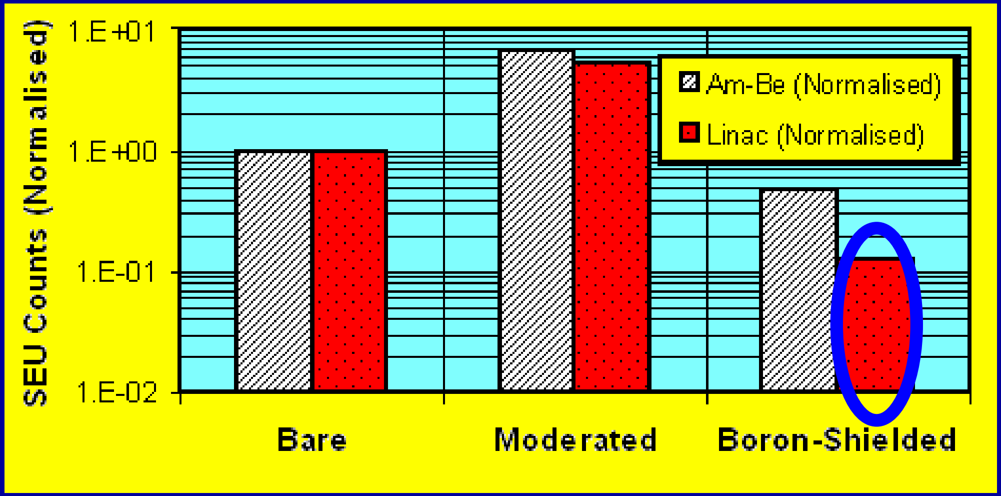

The lowest number SEU in the Poly-Boron shielded SRAMs irradiated at the Linac confirms the existence of a high number of thermal neutrons in the tunnel.

4) REAL TIME SRAM NEUTRON FLUENCE MONITOR

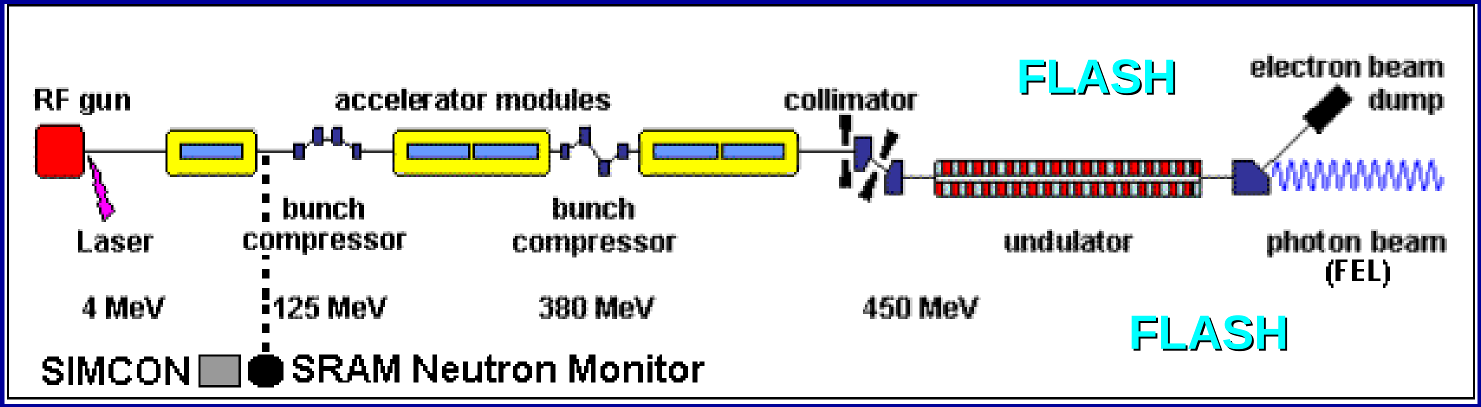

Neutron Monitor, panoramic view
(SMCON Crate located next to monitor)

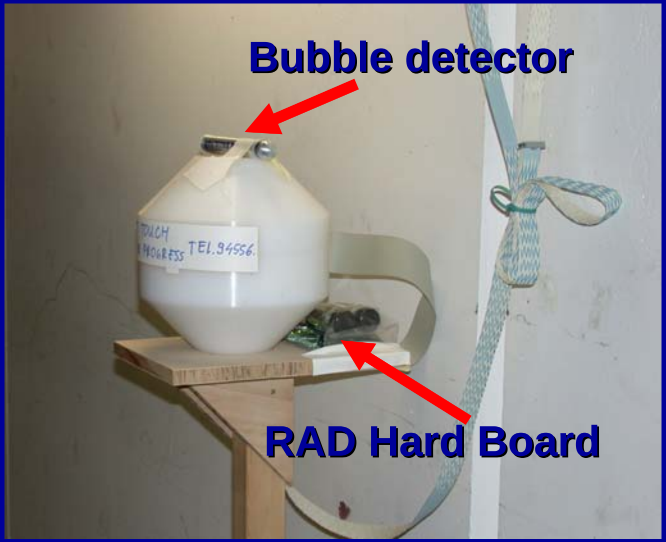

The Moderator, close up view
(Bubble detector for in-situ calibration)

Examples: Effect of Moderator size on monitor sensitivity

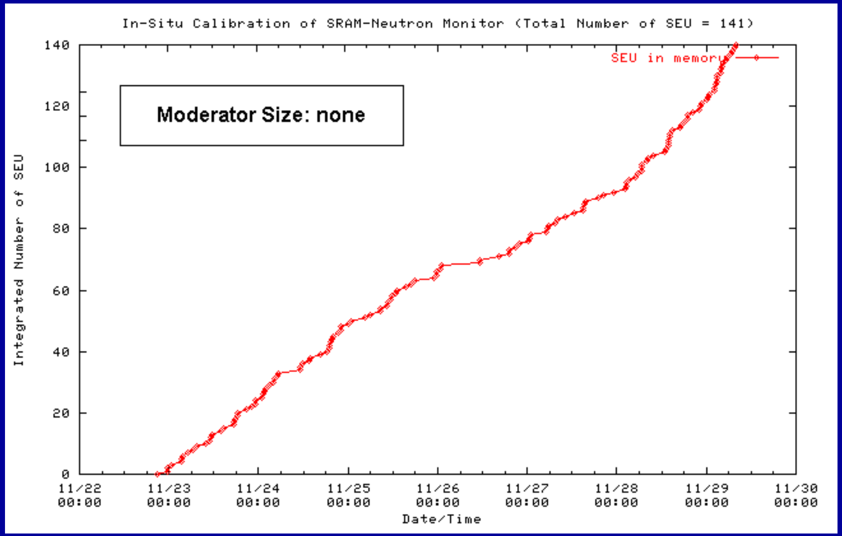

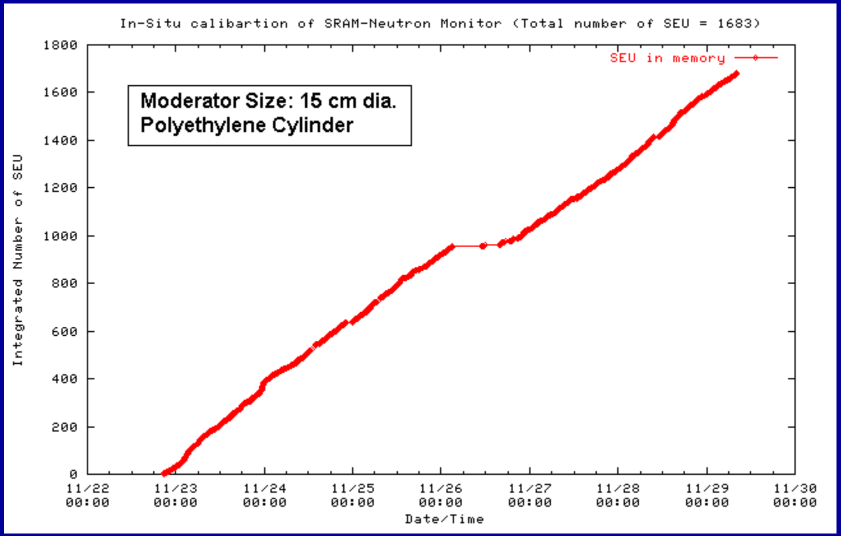

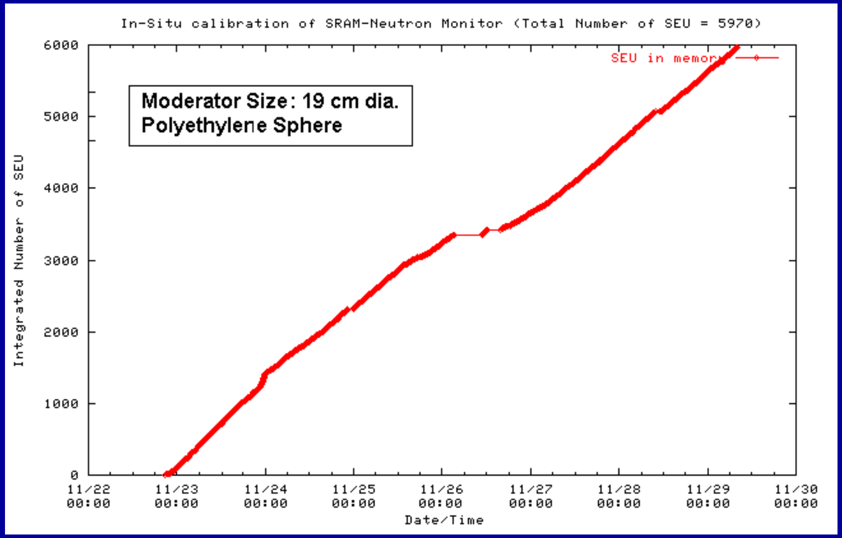

D. Makowski, B. Mukherjee, S. Simrock and others. IEEE Tr. Nucl. Sc. (in press)

D. Makowski, B. Mukherjee, S. Simrock and others. RADEC 2005

D. Makowski, B. Mukherjee, S. Simrock and others. MIXDES 2006

B. Mukherjee, D. Makowski, S. Simrock. Radiat. Prot. Dosim. (under preparation)

5x Real-Time Neutron Monitors will be connected to Doocs Server in July 2006

To see similar plots in real time => **http://neo.dmcs.p.lodz.pl:9999/plot.pl**

APPLICATIONS

Application 1: IN-SITU DOSIMETRY AT FLASH CAVITIES
(Radiation from Field Emission-Dark current)

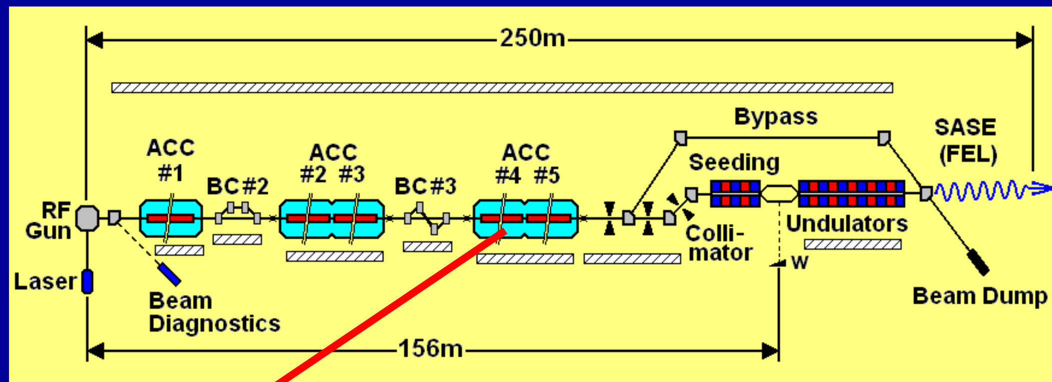

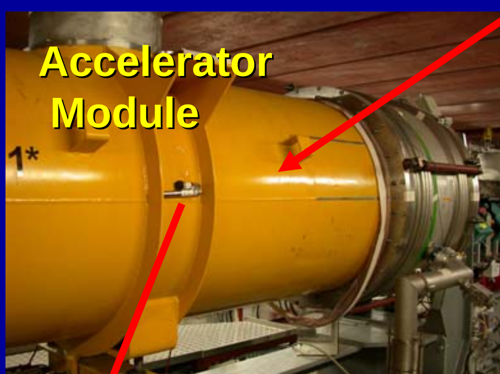

Neutron/Gamma Dosimeter pairs

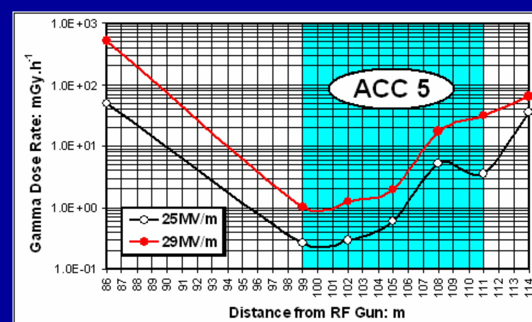

Gamma Dose Rate along the module tank, 0.5m from the module axis evaluated with PorTL (Al_2O_3) TLDs.

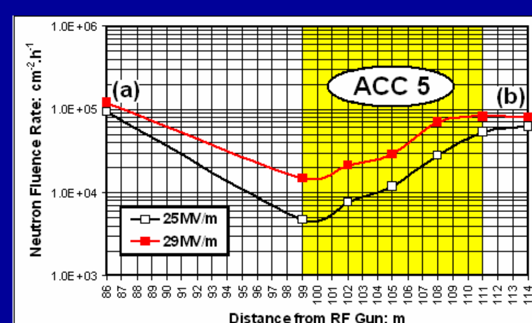

Neutron Fluence Rate along the module tank, 0.5m from the module axis evaluated with BDPND Superheated Emulsion (Bubble) dosimeters.

SUMMARY (Finding)

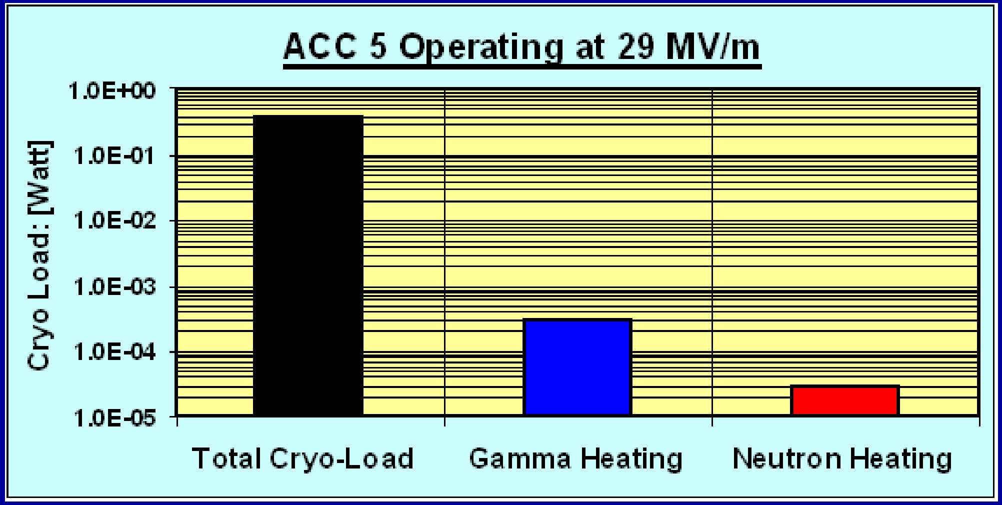

(a) Neutron and gamma radiations are produced when high- energy electrons strike the superconducting Niobium cavities

(b) At 2 ^{o}K, Niobium is superconducting, hence, Ohmic- heat production is nil

(c) Neutrons and gamma rays interact with liquid helium causing Cryo-Load

(d) We have used Al_2O_3 (gammas) and BDPND Bubble detectors (Neutrons) to assess radiation doses (kerma) and then reverse calculated the Cryo (Heat)-Load

Radiation Dose $\Longrightarrow$ Heat Load

Radiation Dose $\cancel{\Longleftarrow}$ Heat Load

Application 2: GaAs LED as High-Level Neutron Dosimeter at FLASH

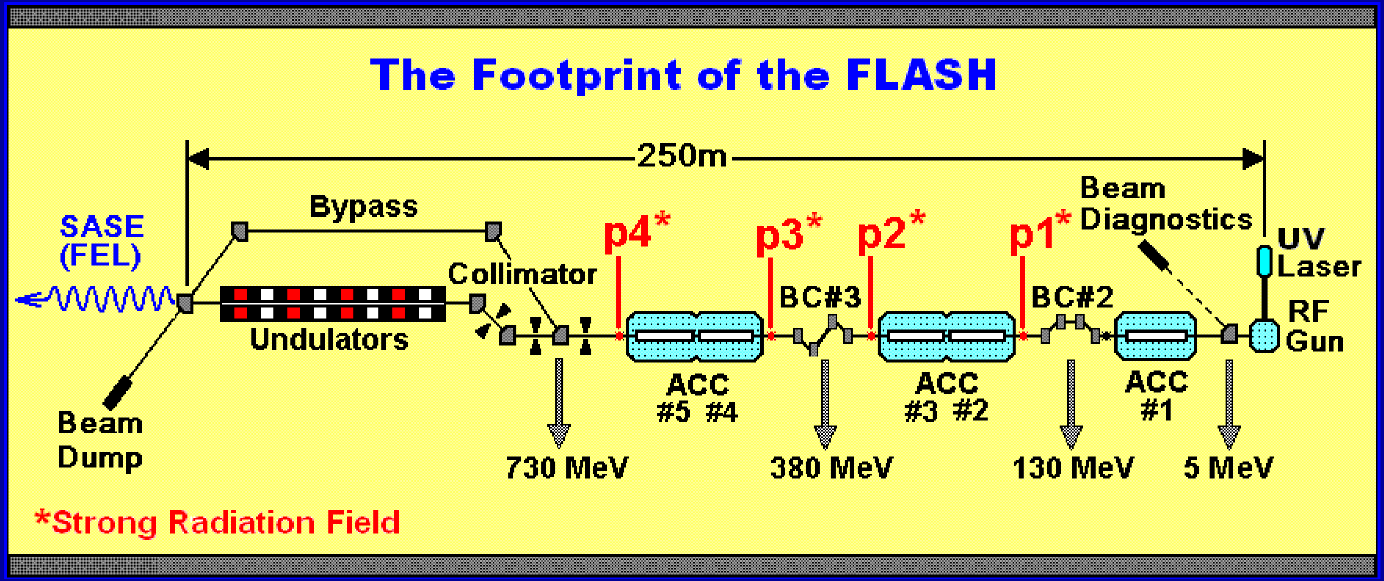

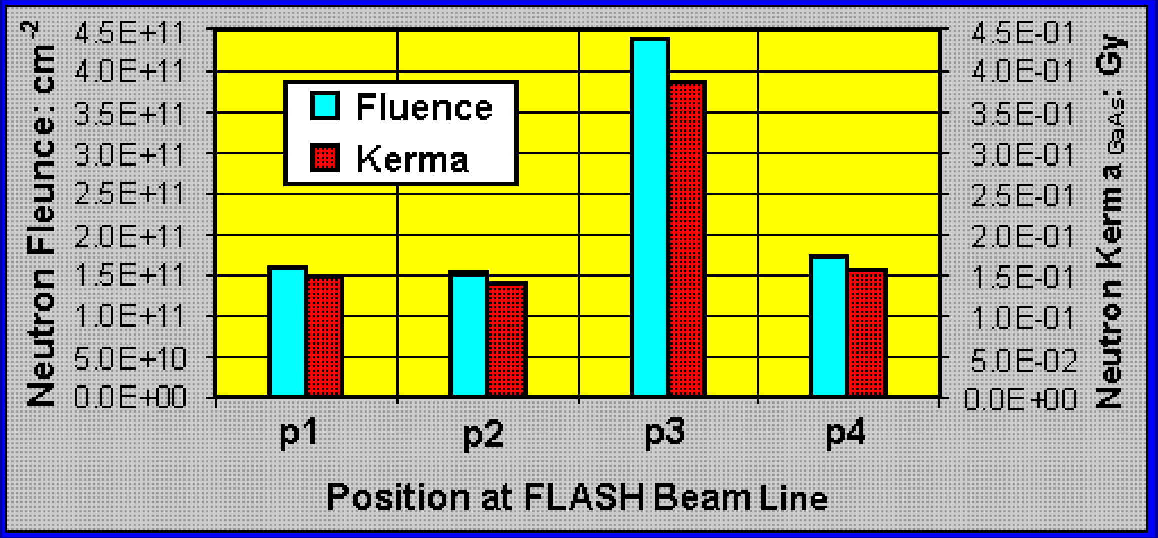

B. Mukherjee, D. Rybka, S. Simrock, Radiat. Prot. Dosim. (Submitted)

Application 3: Interpretation of Anomalous Neutron Production Pattern at ACC 1 using SRAM based Neutron Fluence Monitor

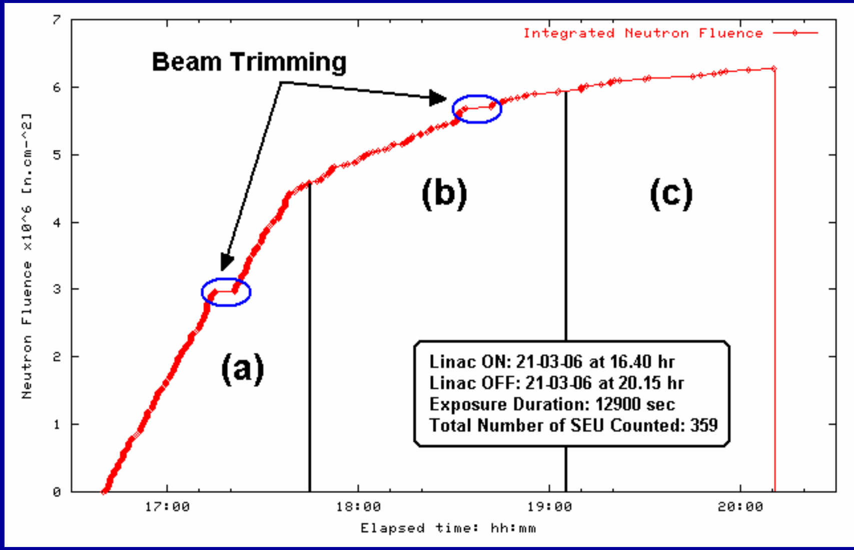

The real-time plot showing the readout of the SRAM neutron detector system. The neutron fluence was evaluated from the SEU in the SRAM Sensor and shown as a function of elapsed time.

Experiment	Duration	Gradient	Pulse length	Collimator
Phase a	16.40 – 17.44	15.5 MV/m	300 micro second	OFF
Phase b	17.44 – 19.13	15.5 MV/m	100 micro second	OFF
Phase c	19.13 – 20.15	15.5 MV/m	100 micro second	ON

TABLE: The SRAM based real-time neutron monitor has proven to be an important tool to analyse the accelerator radiation environment, predominantly caused by dark current of the RF gun. The interpretation of this radiation field reveals important machine operation parameters.

Mitigation Technique

Test Summary of a special purpose Shielding for Microelctronics

Four 512 kB SRAM chips, Unshielded (1), and shielded with Poly-boron (2) , Cadmium (3) and Comp-Mat (4) were exposed to thermal neutron field at FLASH for 4 days.

The SEU in the SRAM chips were counted off-line and are shown in the histogram below.

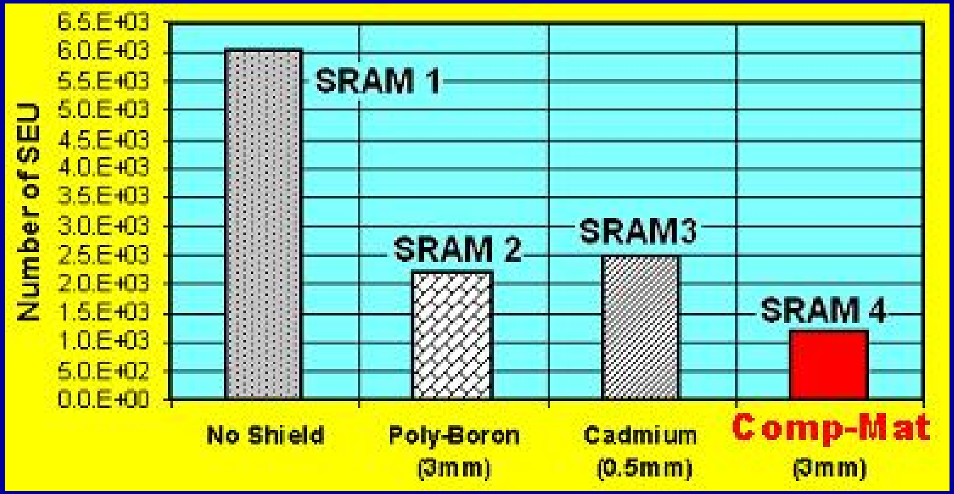

The thermal neutron attenuation coefficient k is defined as the ratio of SEU counts in the shielded and un-shielded SRAMs:

k(Poly-Boron) => 0.36

k(Cadmium) => 0.41

k(Comp-Mat) => 0.20

Evidently, the Comp-Mat outperforms the Poly-Boron Shield (Best thermal neutron shield material available in market) by a factor of 2

SUMMARY AND CONCLUSIONS

This talk highlighted the main research and development activities undertaken during (February 2004 - to date) by the radiation effect project group under the Accelerator Radiation Control (MSK) section of DESY.

OUR MAIN GOALS ARE

Understand the nature of the radiation fields produced by various high-energy particle accelerators operated by Deutsches Elektronen-Synchrotron (DESY) in particular, the Free Electron Laser at Hamburg (FLASH).

Investigate the adverse effects of radiation on microelectronic devices operating the accelerator environment and to find the appropriate mitigation strategy.

Develop Micro and Optoelectronics based radiation detection and measurement devices to cope with the complex nature of the radiation environment of modern particle accelerators.

THANK YOU FOR YOUR PATIENCE

bhaskar.mukherjee@desy.de